Selection of CMIP6 GCM With Projection of Climate Over The Amu Darya River Basin

Obaidullah Salehie
  Universiti Teknologi Malaysia (UTM)

Mohammed Magdy Hamed
  Technology and Maritime Transport (AASTMT)

Tarmizi Ismail (✉ tarmiziismail@utm.my)
  Universiti Teknologi Malaysia (UTM)   https://orcid.org/0000-0002-6748-4703

Tze Huey Tam
  Universiti Teknologi Malaysia

Shamsuddin Shahid
  Universiti Teknologi Malaysia (UTM)

Research Article

Abstract

Global Climate Models (GCMs) are considered the most feasible tools to estimate future climate change. The objective of this study was to assess the interpretation of 19 GCMs of Coupled Model Intercomparison Project 6 (CMIP6) in replicating the historical precipitation and temperature of climate prediction center data for the Amu Darya river basin (ADRB) and the projection of climate of the basin using the selected GCMs. The Kling Gupta efficiency (KGE) metric was used to assess the effectiveness of GCMs to simulate the annual geographic variability of precipitation, maximum and minimum temperature (Pr, Tmx and Tmn). A multi-criteria decision-making approach (MCDMA) was used to integrate the KGE values to rank GCMs. The results revealed that MPI-ESM1-2-LR, CMCC-ESM2, INM-CM4-8 and AWI-CM-1-1-MR are the best in replicating observed Pr, Tmx and Tmn in ADRB. Projection of climate employing the selected GCMs indicated an increase in precipitation (9.9-12.4%) and temperature (1.3-5.5 C) in the basin for all the shared socioeconomic pathways (SSPs), particularly for the far future (2060-2099). A significant variation can be seen in temperature over the different climatic zone. However, the intercomparison of selected GCM projected revealed high uncertainty in the projected climate. The uncertainty is higher in the far future and higher SSPs compared to the near future and lower SSPs.

1. Introduction

Climate change is a worldwide phenomenon that affects almost all aspects of life. The frequency and intensity of climatic hazards have increased globally, which disrupted agricultural livelihoods, water resources, food security, socioeconomic development and human health in many regions (Li et al., 2020a; Pour et al., 2020; Shiru et al., 2020; Wang et al., 2019). However, the impacts of climate change are not consistent throughout the globe. Arid and semi-arid regions are relatively more sensitive than other climate zones due to their vulnerable ecosystem (Ahmed et al., 2019c; Pour et al., 2020). Therefore, due to its arid to semi-arid environment, Central Asia is one of the most exposed areas to climate change (Yadav et al., 2019).

Climate change is generally perceived by studying precipitation and temperature variables (Sheffield and Wood, 2008). Global Climate Models (GCMs) are considered the most feasible tools for simulating the past climate and projection of future climate based on emission scenarios (Li et al., 2020a). Over the years, many GCMs have been developed, and the structure of Coupled Model Intercomparison Project (CMIPs) has been revised from CMIP1 to the newly designed CMIP6 (Meehl et al., 2014; Pascoe et al., 2019; Scher and Messori, 2019). CMIP6 is a set of GCMs and the latest released stage of the CMIP series (Eyring et al., 2016). In addition to the DECK (Diagnostic, Evaluation and Characterization of Klima experiments) and the CMIP6 historical replication, 21 individual MIPs have been endorsed by the CMIP panel for inclusion in CMIP6 (Eyring et al., 2015). The CMIP6 historical simulations consider both anthropogenic and geogenic forcing for the period 1850-2014 (Srivastava et al., 2020). The number of GCMs has increased concerning each generation of MIPs, reaching 55 in CMIP6 (Eyring et al., 2016). In comparison to CMIP5, CMIP6 has numerous advantages that combine RCPs with SSPs, improvements in

the models and additional experiments, higher spatial resolution, less biases, and better representation of synoptic processes (Kamal et al., 2021; Su et al., 2021a).

Multi-model ensembles (MMEs) are usually used to minimize the GCMs uncertainty and generate outputs consistent with local (Ahmed et al., 2019a; Wang et al., 2018). Therefore, choosing a suitable set of GCM is important for better water resource management and climate change impact assessment, especially in developing nations with limited human and computational resources (Hassan et al., 2020; Lin and Tung, 2017). This is because GCMs are not free of biases, either underestimate or overestimate, although the uncertainty is smaller in CMIP6 GCMs than other CMIPs (Srivastava et al., 2020). Selected GCMs should replicate the observed climate in terms of spatial and temporal variability (Nashwan and Shahid, 2020). Generally, a preferable GCM ensemble is selected according to their past performance and the envelope method (Hassan et al., 2020; Salman et al., 2018). The past performance method examines GCMs capability to mimic the past climate without considering the future projection (Raju and Kumar, 2014; Srinivasa Raju and Nagesh Kumar, 2015). The envelope approach selects a set of GCMs models based on probable future climate projections without concerning a GCMs' performance to replicate the historical climate (Warszawski et al., 2014). However, the past performance method is most widely used for GCM ensemble member selection, considering that models able to replicate the observed climate of an area have a better ability to project its future climate (Khan et al., 2020; Nashwan and Shahid, 2020). In literature, different approaches have been offered for GCM selection and ensemble preparation (Hassan et al., 2020; Salman et al., 2018; Shiru et al., 2020).

Several studies assessed climate in central Asia (CA) at the basin, country or regional scale. Duulatov et al. (2019) used 4 GCMs of CMIP5 to assess rainfall changes over CA models for radiative concentration pathways (RCPs) 2.6 and 8.5. Gulakhmadov et al. (2020) used 5 GCMs of CMIP5 to project precipitation (Pr), maximum temperature (Tmx) and minimum temperature (Tmn) in the Vakhsh River Basin of CA for RCP4.5 and RCP8.5. Ta et al. (2018) assessed the performance of 37 GCMs of CMIP5 to mimic historical Pr over CA. Huang et al. (2014) evaluated the ability of 28 GCMs of CMIP5 to project changes in annual Pr over CA for RCPs 2.6 and 8.5. Xiong et al. (2021) assessed the skill of 24 CMIP5 models against climate research unit (CRU) historical temperature in CA. Zhao et al. (2018) used 25 CMIP5 to simulate the subtropical westerly jet and its impact on projected RCP8.5 summer rainfall over CA. Recently, CMIP6 GCMs are also used for climate projections in different parts of CA. Jiang et al. (2020) used 15 CMIP6 models to assess changes in Pr in CA for four shared socioeconomic pathways (SSPs). Li et al. (2020b) used 4 CMIP6 models to evaluate total column water vapor changes in the atmosphere over CA for different SSPs. Guo et al. (2021) assessed the ability of CMIP6 in simulating Pr over CA. Li et al. (2021) used four models of CMIP5 and CMIP6 to project future changes of biodiversity in CA for different RCPs and SSPs.

The Amu Darya River (ADR) is the primary supply of fresh water in CA, and it flows through five countries: Kyrgyzstan, Tajikistan, Afghanistan, Turkmenistan and Uzbekistan (Jalilov et al., 2016). The region's livelihood and national economy depend heavily on water supplies in the ADR basin (Saidmamatov et al., 2020). The basin is highly vulnerable to climate owing to its arid to semi-arid climate and fragile

environment. However, only fewer studies evaluated climate change over the ADR basin. Hagg et al. (2013) used 6 CMIP3 GCMs to project annual and seasonal glacier changes and runoff in the upper ADR basin. White et al. (2014) assessed the ability of fourteen CMIP3 GCMs precipitation and temperature against CRU to project future water supply in the ADR basin. Lutz et al. (2013) evaluated CMIP3 and CMIP5 MME against The Asian Precipitation-Highly-Resolved Observational Data Integration Toward Evaluation (APHRODITE) and Princeton's Global Meteorological Forcing Data (PGMFD) datasets to assess the impact of climate change on the future glacier extent in the ADR and Syr Darya river basins. Su et al. (2021b) developed an integrated multi-GCM Bayesian-neural-network hydrological study using GCM simulated climate to assess the influence of climate change on runoff in the ADR basin. Different studies in the basin and other CA regions used different sets of GCMs, which produced contradictory climate projections. This has also made decision-making based on the previous studies impossible. It is very important to recommend a suitable ensemble for climate projection in the ADR basin. Besides, reliable projection of basin's climate with the selected GCMs for SSPs is vital to aid climate mitigation policymaking.

This study aims to assess CMIP6 GCMs' ability to replicate observed climate in the ADR basin to recommend an appropriate ensemble for the basin's climate projections. Besides, the study projected the basin's climate with associated uncertainty using the selected GCMs to provide vital information required for climate change adaptation planning.

2. Study Area And Data

2.1. Study Area

The Amu Darya River (Figure 1) is the longest river and primary source of fresh water in CA. The river length is 2,540 km, with annual mean flow of about 79 km^3 (Awan et al., 2011; Leng et al., 2021; Schlüter and Herrfahrdt-Pähle, 2011; Wegerich, 2008; Xu et al., 2021). It originated in the high glaciers and snow-covered Hindukush and Pamir mountains in Tajikistan, Kyrgyzstan and Afghanistan, and passed through the deserts and the arid plain in Uzbekistan and Turkmenistan before reaching the Aral Sea (Schlüter and Herrfahrdt-Pähle, 2011; Wang et al., 2021). The average annual rainfall of the basin is 400 mm (Salehie et al., 2021). The topography of the ADR basin ranges from 7,500 m in the upstream mountains to around 200 m in the downstream northwest plains with a delta and feeding the Aral Sea. Some locations in the upstream study area receive rainfall amount nearly 2000 mm, while only 100 mm in the downstream (Behzod and Su-Chin, 2013).

2.2. Gridded data

In this study, the Climate Prediction Center (CPC) data of Pr, Tmx and Tmn for the time horizon of 1979-2014 were used as a reference to estimate the performance of GCMs. CPC is a gauge-based gridded dataset established by the NOAA Climate Prediction Center, National Centers for Environmental Prediction

(Xie et al., 2007). This dataset is available with a spatial resolution of 0.5 ×0.5 from 1979 to present at https://psl.noaa.gov/data/gridded/.

Salehie et al. (2021) assessed the ability of seven gridded precipitation datasets against 55 stations data over the Amu Darya basin. They found that CPC is the best dataset that capable of replicating the observed precipitation. Salehie et al. (2021b) also showed CPC's ability to replicate observed temperature in the basin. Therefore, the CPC dataset was considered the reference dataset used in this study to assess GCMs' performance in simulating Pr, Tmx and Tmn.

2.3. CMIP6 GCMs simulations and scenarios

Nineteen CIMP6 GCMs monthly Pr, Tmx and Tmn simulations were used to select the best GCMs to replicate the rainfall in the study area. Several international research organizations collaborated to produce these GCMs is presented in Table S-1. The GCMs were chosen based on the availability of monthly historical simulation and future projections for four SSPs, namely SSPs (1-2.6, 2-4.5, 3-7.0 and 5-8.5). For a fair comparison of various GCMs model, historical single run r1i1p1f1 (e.g., ensemble members [r1], initialization states [i1], physical parameterizations [p1] and forcing index [f1]) were considered for all cases. GCMs' historical (1979-2014) and projection (2015-2100) data could be downloaded from this website: http://cmip-pcmdi.llnl.gov/ cmip6/.

3. Methodology

The reference dataset (CPC) and GCMs have various spatial resolutions. Hence, CPC, historical and future projection GCMs were interpolated to 73 grid points having the common 1°×1° resolution for all variables (Pr, Tmx and Tmn). This resolution was chosen as it was almost close to the mean of all GCMs. The inverse distance weighting approach was used to interpolate the four closest grid points to each grid point, as discussed in (Hamed et al., 2021). GCMs were re-gridding to prevent bias from different spatial resolutions during performance evaluation (Nashwan and Shahid, 2020). The procedures for the selection of GCMs are defined below:

1. Compare the monthly historical variables of 19 GCMs and the reference dataset (CPC) using the KGE metric at each grid point.
2. Rank each variable based on KGE, then select the GCM subset using the multi-criteria decision analysis (MCDMA) method.
3. Create an MME using the top four GCMs results from the ranking process.
4. Use the MME to project all climate variables in the near and far future.

3.1 Performance evaluation using KGE

In this study, Kling-Gupta efficiency (KGE) was used to evaluate the performance of the historical GCMs in replicating the observed dataset in three different variables (Pr, Tmx and Tmn). KGE is a statistical index incorporating correlation, bias, and variability to find the association and biases in the mean and the

changes of measured and predicted climate variables (Nashwan and Shahid, 2020). KGE was presented by Gupta et al. (2009) and then modified by Kling et al. (2012), which defined as:

$$KGE = 1 - \sqrt{(r - 1)^2 + (\beta - 1)^2 + (\gamma - 1)^2}$$ Equation 1

where r is the linear correlation between observed and gridded data; β represents the bias obtained by the ratio of mean simulated and mean observed and   is the variability component can be calculated by the percentage of the simulated (GCMs) and observed (CPC) coefficients of variation:

$$\beta = \frac{\mu_s}{\mu_0} \quad and \quad \gamma = \frac{\sigma_s/\mu_s}{\sigma_0/\mu_0}$$ Equation 2

where μ and σ are the distribution mean and standard deviation, respectively, while the subscripts s and o reflect simulated and observed data, respectively. KGE can range between $-\infty$ to 1, where 1 is the optimal value.

3.2 Ranking of GCMs

Multi-criteria decision making analysis (MCDMA) is a recall for evaluating an alternative from multi-objective complex problems, uncertain information of physical and social issues when no method is found to undertake (Wang et al., 2009). MCDMA approach integrates statistically and numerically obtained outcomes to rank the best option of different choices (Salehie et al., 2021). In this study, the GCMs are ranked using the KGE metric in a different variable based on their performance. The higher weight to a GCM model is provided as a higher frequency of occurrence, and therefore the models top-ranked. For example, if the model ranked first at most grids from the total number of grid points for each variable, it shall be ranked the first among all GCMs. The output rank from each variable was merged using the average method as shown in Equation 3. Finally, the average sum was ranked to describe the best GCMs among the set.

$$Average\ Sum = \frac{Pr_{rank} + Tmx_{rank} + Tmn_{rank}}{3}$$ Equation 3

3.3 Ensemble projections

The top four GCMs were used to create an ensemble mean for climate projection. The advantages of MME are increasing the accuracy of projection and reducing uncertainty in the individual model (Ahmed et al., 2020; Salman et al., 2018; Shiru et al., 2020). Different techniques are used to generate MME, but the most commonly used is the weighted average method (Sachindra et al., 2014; Shiru et al., 2020). This technique was also adopted in the current study. The MME was used to project the ADR basin's climate change for two periods; the near future (2020-2059) and the far future (2060-2099). Spatial distribution

maps were created to show the change in the basin for precipitation (%) and temperature (C). Also, the change that happened in each climate zone were presented for each variable.

4. Results

4.1. Mean annual precipitation spatial distribution

The mean annual precipitation climatology of CPC and 19 GCMs of CMIP6 for the period of 1979-2014 are presented in Figure 2, while the mean Tmx and Tmn were shown in S-1 and S-2 in the supplementary. CPC showed that the mean annual precipitation for the study area ranged between 50 and 350 mm. The highest precipitation occurs in the center part, while the lowest is in the basin's northwest. The precipitation decreases gradually from south of Tajikistan and north of Afghanistan until it reaches the basin's northwest. It was observed from the figure that some GCMs such as EC-Earth3-Veg and EC-Earth3-Veg-LR shows similar spatial pattern to observed precipitation. Many GCMs like ACCESS-CM2, ACCESS-ESM1-5 and BCC-CSM2-MR showed high precipitation in the center and east part of the basin, while INM-CM4-8 and INM-CM5-0 showed relatively less precipitation in the center of the basin.

4.2. Performance evaluation of GCMs

The GCM's performance was evaluated against CPC precipitation, Tmx and Tmn data for the period 1979-2014 using the KGE metric. The results are presented using a level plot in Figure 3. The median of KGE for all GCMs for annual Pr, Tmx and Tmn were -0.03, 0.51 and -1.37, respectively. Both Pr and Tmn gave a negative KGE value for many GCMs, while GCMs' Tmx showed a high ability to replicate the CPC Tmx. The results showed the highest KGE value (0.85) for INM-CM4-8 in Tmx and the lowest, 0.11, for EC-Earth3-Veg for Pr.

4.3. Ranking of GCMs

Based on KGE values for each GCM, the GCMs were ranked for each variable in ascending order from the highest KGE to the lowest value. The higher value of KGE for a GCM indicates its better skill in replicating historical observations. The average rank of all three variables was obtained using Equation 3, as shown in Table 1. Finally, the lowest average rank was taken as the best GCM in reproducing the CPC dataset. The results indicate that MPI-ESM1-2-LR, CMCC-ESM2, INM-CM4-8 and AWI-CM-1-1-MR ranked 1st, 2nd, 3rd, and 4th, respectively. The rest of the GCMs showed weak performance in replicating the observations. The top four GCMs were taken as an ensemble mean to represent the observed data for climate projection.

Table 1
KGE ranking of GCMs and the final rank using MCDMA

GCMs	Rank (Pr)	Rank (Tmx)	Rank (Tmn)	Average Sum	MCDMA
ACCESS-CM2	7	12	7	8.67	6
ACCESS-ESM1-5	19	6	1	8.67	7
AWI-CM-1-1-MR	4	8	12	8	**4**
BCC-CSM2-MR	14	7	17	12.67	16
CanESM5	11	9	9	9.67	10
CMCC-CM2-SR5	8	17	6	10.33	11
CMCC-ESM2	9	5	4	6	**2**
EC-Earth3	3	13	19	11.67	15
EC-Earth3-Veg	1	15	15	10.33	12
EC-Earth3-Veg-LR	2	16	16	11.33	14
FGOALS-g3	16	19	8	14.33	17
GFDL-ESM4	13	14	18	15	18
INM-CM4-8	5	1	14	6.67	**3**
INM-CM5-0	12	2	11	8.33	5
IPSL-CM6A-LR	18	18	10	15.33	19
MIROC6	15	10	3	9.33	9
MPI-ESM1-2-HR	10	4	13	9	8
MPI-ESM1-2-LR	6	3	2	3.67	**1**
MRI-ESM2-0	17	11	5	11	13

4.4. Climate projection

The top selected GCMs were merged to create the mean MME. The MME was used to project the changes in annual Pr, Tmx and Tmn for four SSPs in the near future (2020-2059) and the far future (2060-2099) over different climate zones of the basin. The map of climate zones is presented in Figure 4, which was adapted from the Köppen-Geiger climate classification global map (Peel et al., 2007). The following sections summarize the projected fluctuations in annual Pr, Tmx and Tmn.

4.4.1. Precipitation projection

The changes for Pr in the ADR basin projected by MME of the selected GCMs are presented in Figure 5. Results indicate that projected change in the far future is higher (3.3-12.5 %) than in the near future for all SSPs. The percentage of change in Pr in the near future for SSP1-2.6 to SSP5-8.5 were in the range of -12.4 to 3.1%, -7.3 to 10.5%, -6.4 to 7.0% and -10.3 to 4.2%. The projected change in Pr for the far futures for those SSPs were -8.3 to 3.3%, 1.6 to 9.1%, -4.2 to 12.2% and -4.3 to 10.8%. Most GCMs projected higher Pr over a small patch in the northwest cold desert climate region. This increase in Pr could be due to the effect of atmospheric circulation of the Caspian Sea due to increased temperature (Farley Nicholls and Toumi, 2014). It could also be due to the effect of the Aral Sea surrounding the delta of the ADR basin. The highest precipitation in the east part of the basin may be due to the Siberian monsoon in winter and spring that fall as rain and snow (Wang et al., 2020). From SSP1-2.6 for the near future, it can be seen that the rainfall change is negative in most parts of the basin with harsh change in the center to south part. However, this scenario shows the negative change for the far future over the basin but relatively less compared to that in the near future.

4.4.2. Temperature projection

The annual Tmx changes were presented as the absolute difference between the future projection and the historical simulation. The geographical distribution in the changes of annual Tmx is presented in Figure 6. The figure indicates a gradual increase in Tmx from SSP1-2.6 to 5-8.5 across the basin for both the future periods. However, all GCMs showed a greater increase for the far future compared to the near future. Only SSP3-7.0 showed a homogeneous spatial distribution of Tmx over the whole basin. The lower projected change in Tmx in the near future was from 1.3 to1.6 C, while the far future ranged between 1.6 and 4.9 C. The highest increase (4.9 C) was for far future SSP5-8.5.

The changes in annual Tmn were very similar to Tmx. The spatial patterns of the projected change in Tmn are presented in Figure 7. Compared to Tmx, the projected change in Tmn was higher. There was a variation in change for different GCMs, except for SSP5-8.5 in the near future, which showed a more homogenous spatial pattern in change for all GCMs. Like Tmx, a gradual increase in Tmn was noticed from SSP1-2.6 to 5-8.5 across the basin for both future scenarios. The higher increase was projected for the far future in the range of 2.3–5.5 C. The highest increase in Tmn (5.5 C) was for SSP5-8.5 in the far future, while the lowest change (1.3 C) was for near future SSP1-2.6.

4.5. Uncertainty in projected climate change

The uncertainty in the projected climate was estimated from the lower and upper band values of projections by different GCMs for individual SSP. The uncertainty in the projected Pr in different climate zones for different SSPs are shown in Figure 8. It shows a higher uncertainty in projection in the far future (2060-2100) compared to the near future (2020-2059). The uncertainty in projection was also higher for higher SSPs. For example, the highest upper band value (32%) was observed for far future SSP5-8.5.

Uncertainties associated with Tmx are presented in Figure 9. Uncertainty in Tmx was less compared to Pr. The variation in projection was in the range of 3.0 to 7.0°C or 4.0°C for climate zone 4 (Warm Dry Summer Continental Climate). Similarly, the uncertainty in the projected Tmn (Figure 10) was less. The

highest uncertainty in Tmn was 3.8°C for SSP5-8.5 during 2060-2099 for climate zone 1 (Cold Desert Climate). However, like Pr, the uncertainty for both Tmx and Tmn was higher for the far future and higher SSPs.

5. Discussion

Different GCMs models have a degree of uncertainty (Khan et al., 2020; Lutz et al., 2016). Therefore, it is important to select GCMs based on their performance in modeling the climatic of an area to decrease the uncertainty of the climate projection (Ahmed et al., 2019b; Salman et al., 2018). MMEs are usually suggested to decrease the uncertainties related to GCMs simulations or projections (Ahmed et al., 2020). In this study, we used the past performance approach to choose a subset of GCMs (MME) to reduce uncertainties related to the individual model.

Few studies have been conducted in the ADR basin, which is different from our work in terms of method and data availability. A recent study (Guo et al., 2021) used CMIP6 to simulate precipitation over CA found that the performance of GCMs varies from region to region with a consistent annual cycle shape in western CA. They showed limited models performance in simulating the observations. White et al. (2014) used mean MME SRA2 precipitation annual temperature anomalies for 2070-2099 over the ADR basin. They showed a mean annual rise in temperature ranged between 4 and 4.6°C through the basin by 2070-2099 under a high-emission scenario and downward precipitation trend, ranging between –5.3% in Nukus city Uzbekistan and -13.6% in Mary city in the Karakum desert Turkmenistan. Xu et al. (2021) projected streamflow in ADR for climate change scenarios. The multi-scenario ensemble streamflow forecast showed that during 2021-2050, the mean annual precipitation and the mean temperature should increase. However, the average annual streamflow would decline, which climate change donates 78.8–98.7% of streamflow change in each scenario.

This study used the past performance approach to select a subset of GCMs from 19 GCMs. Secondly, the KGE metric was used to assess the association between all GCMs and the CPC (Pr, Tmx and Tmn) at each of the 73 grid points of 1°×1° resolution. Thirdly, an MCDMA was used to rank the inconsistent results obtained using KGE for three variables (Pr, Tmx and Tmn). The results of MCDMA revealed that MPI-ESM1-2-LR, CMCC-ESM2, INM-CM4-8 and AWI-CM-1-1-MR are the best in replicating observed climate in ADRB.

Results obtained using future MMEs showed an increase in Pr ranged between 3.3 and 12.5% in the far future (2060-2099) when all SSPs were considered. The four SSPs' spatial pattern of projected change showed a higher increase in Pr in the east and northwest of the basin and less in the basin's centre. This result contradicts Agal'tseva et al. (2010) findings, which showed a 5-12% reduction in precipitation during 2070-2099.

The absolute change in temperature between the historical and future projection MME were used to present the change in Tmx and Tmn. The results indicated a gradual increase in Tmx and Tmn in the

basin. The results were almost in agreement with that reported in previous studies (Agal'tseva et al., 2010; Gulakhmadov et al., 2020; White et al., 2014; Xu et al., 2021) in the region.

6. Conclusions

The performance of 19 GCM-CMIP6 in replicating the historical precipitation and temperature in the ADR basin was assessed to recommend an appropriate set of GCMs for climate studies. Besides, the study employed the selected GCMs for the projection of the climate of the basin for different SSPs with associated uncertainty. The results showed that MPI-ESM1-2-LR, CMCC-ESM2, INM-CM4-8 and AWI-CM-1-1-MR are the best in replicating observed Pr, Tmx and Tmn in the ADR basin. Climate projection using the selected GCMs revealed a rise in Pr, Tmx and Tmn in the basin for all SSPs, especially for 2060-2099. A rise in both precipitation and temperature was projected higher for higher SSPs and more in the far future compared to the near future. The uncertainty in projected climate showed more uncertainty in precipitation projections compared to temperature. The uncertainty was also noticed higher for higher SSPs and in the far future compared to the near future. This is the first attempt to evaluate CMIP6 GCMs' performance in the ADR basin to select the GCM ensemble and climate projections using the selected ensemble. The results of the study can be used for climate change studies and decision-making processes. In the future, GCMs' skills can be evaluated according to the ability to replicate climatic extremes in the basin. Besides, the selected GCMs can be used to evaluate future changes in climate extremes, like floods and droughts in the basin.

Declarations

Conflict of interest

The authors declare no conflict of interest.

Availability of data:

All the data are available in the public domain at the links provided in the texts

Availability of code

The codes used for the processing of data can be provided on request to the corresponding author.

Ethics approval

Not Applicable

Consent to participate

Not Applicable

Consent for publication

All the authors consented to publish the paper

Authors contribution

All the authors contributed to conceptualizing and designing the study. Obaidullah Salehie and Tarmizi bin Ismail gathered data; the programming code was written by Shamsuddin Shahid and Mohammed Magdy Hamed; the initial draft of the paper was prepared by Obaidullah Salehie and Tze Huey Tam; the article was repeatedly revised to generate the final version by Tarmizi bin Ismail and Shamsuddin Shahid.

References

1. Agal'tseva N, Spectorman T, White C, Tanton T (2010) Modelling the future climate of the Amu Darya Basin. *Interstate Water Resource Risk Management: Towards a sustainable future for the Aral Basin,IWA Publishing*,9–32

2. Ahmed K, Sachindra D, Shahid S, Iqbal Z, Nawaz N, Khan N (2020) Multi-model ensemble predictions of precipitation and temperature using machine learning algorithms. Atmos Res 236:104806

3. Ahmed K, Sachindra DA, Shahid S, Demirel MC, Chung E-S (2019a) Selection of multi-model ensemble of GCMs for the simulation of precipitation based on spatial assessment metrics. *Hydrology and Earth System Sciences Discussions*

4. Ahmed K, Shahid S, Sachindra D, Nawaz N, Chung E-S (2019b) Fidelity assessment of general circulation model simulated precipitation and temperature over Pakistan using a feature selection method. J Hydrol 573:281–298

5. Ahmed K, Shahid S, Wang X, Nawaz N, Khan N (2019c) Spatiotemporal changes in aridity of Pakistan during 1901–2016. Hydrol Earth Syst Sci 23(7):3081–3096

6. Awan UK, Tischbein B, Conrad C, Martius C, Hafeez M (2011) Remote sensing and hydrological measurements for irrigation performance assessments in a water user association in the lower Amu Darya River Basin. Water Resour Manage 25(10):2467–2485

7. Behzod G, Su-Chin C (2013) Water salinity changes of the gauging stations along the Amu Darya River

8. Duulatov E, Chen X, Amanambu AC, Ochege FU, Orozbaev R, Issanova G, Omurakunova G (2019) Projected rainfall erosivity over Central Asia based on CMIP5 climate models. Water 11(5):897

9. Eyring V, Bony S, Meehl G, Senior C, Stevens B, Stouffer R, Taylor K (2015) Overview of the Coupled Model Intercomparison Project Phase 6 (CMIP6) experimental design and organization.*Geoscientific Model Development Discussions*, *8*(12)

10. Eyring V, Bony S, Meehl GA, Senior CA, Stevens B, Stouffer RJ, Taylor KE (2016) Overview of the Coupled Model Intercomparison Project Phase 6 (CMIP6) experimental design and organization. Geosci Model Dev 9(5):1937–1958

11. Farley Nicholls J, Toumi R (2014) On the lake effects of the Caspian Sea. Q J R Meteorol Soc 140(681):1399–1408

12. Gulakhmadov A, Chen X, Gulahmadov N, Liu T, Anjum MN, Rizwan M (2020) Simulation of the potential impacts of projected climate change on streamflow in the Vakhsh river basin in central Asia under CMIP5 RCP scenarios. Water 12(5):1426

13. Guo H, Bao A, Chen T, Zheng G, Wang Y, Jiang L, De Maeyer P (2021) Assessment of CMIP6 in simulating precipitation over arid Central Asia. Atmos Res 252:105451

14. Gupta HV, Kling H, Yilmaz KK, Martinez GF (2009) Decomposition of the mean squared error and NSE performance criteria: Implications for improving hydrological modelling. J Hydrol 377(1–2):80–91

15. Hagg W, Hoelzle M, Wagner S, Mayr E, Klose Z (2013) Glacier and runoff changes in the Rukhk catchment, upper Amu-Darya basin until 2050. Glob Planet Change 110:62–73

16. Hamed MM, Nashwan MS, Shahid S (2021) Performance evaluation of reanalysis precipitation products in Egypt using fuzzy entropy time series similarity analysis.*International Journal of Climatology*

17. Hassan I, Kalin RM, White CJ, Aladejana JA (2020) Selection of CMIP5 GCM ensemble for the projection of Spatio-temporal changes in precipitation and temperature over the Niger Delta, Nigeria. Water 12(2):385

18. Huang A, Zhou Y, Zhang Y, Huang D, Zhao Y, Wu H (2014) Changes of the annual precipitation over central Asia in the twenty-first century projected by multimodels of CMIP5. J Clim 27(17):6627–6646

19. Jalilov S-M, Keskinen M, Varis O, Amer S, Ward FA (2016) Managing the water–energy–food nexus: Gains and losses from new water development in Amu Darya River Basin. J Hydrol 539:648–661

20. Jiang J, Zhou T, Chen X, Zhang L (2020) Future changes in precipitation over Central Asia based on CMIP6 projections. Environmental Research Letters 15(5):054009

21. Kamal AM, Hossain F, Shahid S (2021) Spatiotemporal Changes in Rainfall and Droughts of Bangladesh for 1.5 ° and 2°c Temperature Rise Scenarios of CMIP6 Models.

22. Khan N, Shahid S, Ahmed K, Wang X, Ali R, Ismail T, Nawaz N (2020) Selection of GCMs for the projection of spatial distribution of heat waves in Pakistan. Atmos Res 233:104688

23. Kling H, Fuchs M, Paulin M (2012) Runoff conditions in the upper Danube basin under an ensemble of climate change scenarios. J Hydrol 424:264–277

24. Leng P, Zhang Q, Li F, Kulmatov R, Wang G, Qiao Y, Zhu N (2021) Agricultural impacts drive longitudinal variations of riverine water quality of the Aral Sea basin (Amu Darya and Syr Darya Rivers), Central Asia. Environ Pollut 284:117405

25. Li J, Chen X, Kurban A, Van de Voorde T, De Maeyer P, Zhang C (2021) Coupled SSPs-RCPs scenarios to project the future dynamic variations of water-soil-carbon-biodiversity services in Central Asia. Ecol Ind 129:107936

26. Li Z, Li Q, Wang J, Feng Y, Shao Q (2020a) Impacts of projected climate change on runoff in upper reach of Heihe River basin using climate elasticity method and GCMs. Sci Total Environ 716:137072

27. Li Z, Tao H, Hartmann H, Su B, Wang Y, Jiang T (2020b) Variation of projected atmospheric water vapor in central Asia using multi-models from CMIP6. Atmosphere 11(9):909

28. Lin C-Y, Tung C-P (2017) Procedure for selecting GCM datasets for climate risk assessment. *Terrestrial, Atmospheric & Oceanic Sciences*, *28*(1)

29. Lutz AF, Immerzeel WW, Gobiet A, Pellicciotti F, Bierkens MF (2013) Comparison of climate change signals in CMIP3 and CMIP5 multi-model ensembles and implications for Central Asian glaciers. Hydrol Earth Syst Sci 17(9):3661–3677

30. Lutz AF, Maat ter, Biemans HW, Shrestha H, Wester AB, Immerzeel WW (2016) Selecting representative climate models for climate change impact studies: an advanced envelope-based selection approach. Int J Climatol 36(12):3988–4005

31. Meehl GA, Moss R, Taylor KE, Eyring V, Stouffer RJ, Bony S, Stevens B (2014) Climate model intercomparisons: Preparing for the next phase. Eos, Transactions American Geophysical Union 95(9):77–78

32. Nashwan MS, Shahid S (2020) A novel framework for selecting general circulation models based on the spatial patterns of climate. Int J Climatol 40(10):4422–4443

33. Pascoe C, Lawrence BN, Guilyardi E, Juckes M, Taylor KE (2019) Designing and documenting experiments in CMIP6. *Geosci. Model Dev. Discuss*

34. Peel MC, Finlayson BL, McMahon TA (2007) Updated world map of the Koppen-Geiger climate classification. Hydrol Earth Syst Sci 11(5):1633–1644

35. Pour SH, Wahab A, Shahid S (2020) Spatiotemporal changes in aridity and the shift of drylands in Iran. Atmos Res 233:104704

36. Raju KS, Kumar DN (2014) Ranking of global climate models for India using multicriterion analysis. Climate Res 60(2):103–117

37. Sachindra D, Huang F, Barton A, Perera B (2014) Multi-model ensemble approach for statistically downscaling general circulation model outputs to precipitation. Q J R Meteorol Soc 140(681):1161–1178

38. Saidmamatov O, Rudenko I, Pfister S, Koziel J (2020) Water–energy–food nexus framework for promoting regional integration in Central Asia. Water 12(7):1896

39. Salehie O, Ismail T, Shahid S, Ahmed K, Adarsh S, Asaduzzaman M, Dewan A (2021) Ranking of gridded precipitation datasets by merging compromise programming and global performance index: a case study of the Amu Darya basin.*Theoretical and Applied Climatology*,1–15

40. Salman SA, Shahid S, Ismail T, Ahmed K, Wang X-J (2018) Selection of climate models for projection of spatiotemporal changes in temperature of Iraq with uncertainties. Atmos Res 213:509–522

41. Scher S, Messori G (2019) Weather and climate forecasting with neural networks: using general circulation models (GCMs) with different complexity as a study ground. Geosci Model Dev 12(7):2797–2809

42. Schlüter M, Herrfahrdt-Pähle E (2011) Exploring resilience and transformability of a river basin in the face of socioeconomic and ecological crisis: an example from the Amudarya River basin, central Asia.*Ecology and Society*, *16*(1)

43. Sheffield J, Wood EF (2008) Projected changes in drought occurrence under future global warming from multi-model, multi-scenario, IPCC AR4 simulations. Clim Dyn 31(1):79–105

44. Shiru MS, Chung E-S, Shahid S, Alias N (2020) GCM selection and temperature projection of Nigeria under different RCPs of the CMIP5 GCMS. Theoret Appl Climatol 141(3):1611–1627

45. Srinivasa Raju K, Kumar N, D (2015) Ranking general circulation models for India using TOPSIS. Journal of Water and Climate Change 6(2):288–299

46. Srivastava A, Grotjahn R, Ullrich PA (2020) Evaluation of historical CMIP6 model simulations of extreme precipitation over contiguous US regions. Weather and Climate Extremes 29:100268

47. Su B, Huang J, Mondal SK, Zhai J, Wang Y, Wen S, Jiang T (2021a) Insight from CMIP6 SSP-RCP scenarios for future drought characteristics in China. Atmos Res 250:105375

48. Su Y, Li Y, Liu Y, Huang G, Jia Q, Li Y (2021b) An integrated multi-GCMs Bayesian-neural-network hydrological analysis method for quantifying climate change impact on runoff of the Amu Darya River basin. Int J Climatol 41(5):3411–3424

49. Ta Z, Yu Y, Sun L, Chen X, Mu G, Yu R (2018) Assessment of precipitation simulations in Central Asia by CMIP5 climate models. Water 10(11):1516

50. Wang B, Zheng L, Liu DL, Ji F, Clark A, Yu Q (2018) Using multi-model ensembles of CMIP5 global climate models to reproduce observed monthly rainfall and temperature with machine learning methods in Australia. Int J Climatol 38(13):4891–4902

51. Wang J-J, Jing Y-Y, Zhang C-F, Zhao J-H (2009) Review on multi-criteria decision analysis aid in sustainable energy decision-making. Renew Sustain Energy Rev 13(9):2263–2278

52. Wang M, Chen X, Sidike A, Cao L, DeMaeyer P, Kurban A (2021) Optimal Allocation of Surface Water Resources at the Provincial Level in the Uzbekistan Region of the Amudarya River Basin. Water 13(11):1446

53. Wang R, Cheng Q, Liu L, Yan C, Huang G (2019) Multi-model projections of climate change in different RCP scenarios in an arid inland region, Northwest China. Water 11(2):347

54. Wang T, Li T-Y, Zhang J, Wu Y, Chen C-J, Huang R, Artemevna Blyakharchuk T (2020) A Climatological Interpretation of Precipitation δ18O across Siberia and Central Asia. Water 12(8):2132

55. Warszawski L, Frieler K, Huber V, Piontek F, Serdeczny O, Schewe J (2014) The inter-sectoral impact model intercomparison project (ISI–MIP): project framework. *Proceedings of the National Academy of Sciences, 111*(9), 3228-3232

56. Wegerich K (2008) Hydro-hegemony in the Amu Darya basin. Water Policy 10(S2):71–88

57. White CJ, Tanton TW, Rycroft DW (2014) The impact of climate change on the water resources of the Amu Darya Basin in Central Asia. Water Resour Manage 28(15):5267–5281

58. Xie P, Chen M, Yang S, Yatagai A, Hayasaka T, Fukushima Y, Liu C (2007) A gauge-based analysis of daily precipitation over East Asia. J Hydrometeorol 8(3):607–626

59. Xiong Y, Ta Z, Gan M, Yang M, Chen X, Yu R, Yu Y (2021) Evaluation of cmip5 climate models using historical surface air temperatures in central Asia. Atmosphere 12(3):308

60. Xu Z, Li Y, Huang G, Wang S, Liu Y (2021) A multi-scenario ensemble streamflow forecast method for Amu Darya River Basin under considering climate and land-use changes. J Hydrol 598:126276

61. Yadav SS, Hegde V, Habibi AB, Dia M, Verma S (2019) Climate change, agriculture and food security. *Food Security and Climate Change; Yadav, SS, Redden, RJ, Hatfield, JL, Ebert, AW, Hunter, D., Eds*

62. Zhao Y, Yu X, Yao J, Dong X (2018) Evaluation of the subtropical westerly jet and its effects on the projected summer rainfall over central Asia using multi-CMIP5 models. Int J Climatol 38:e1176–e1189
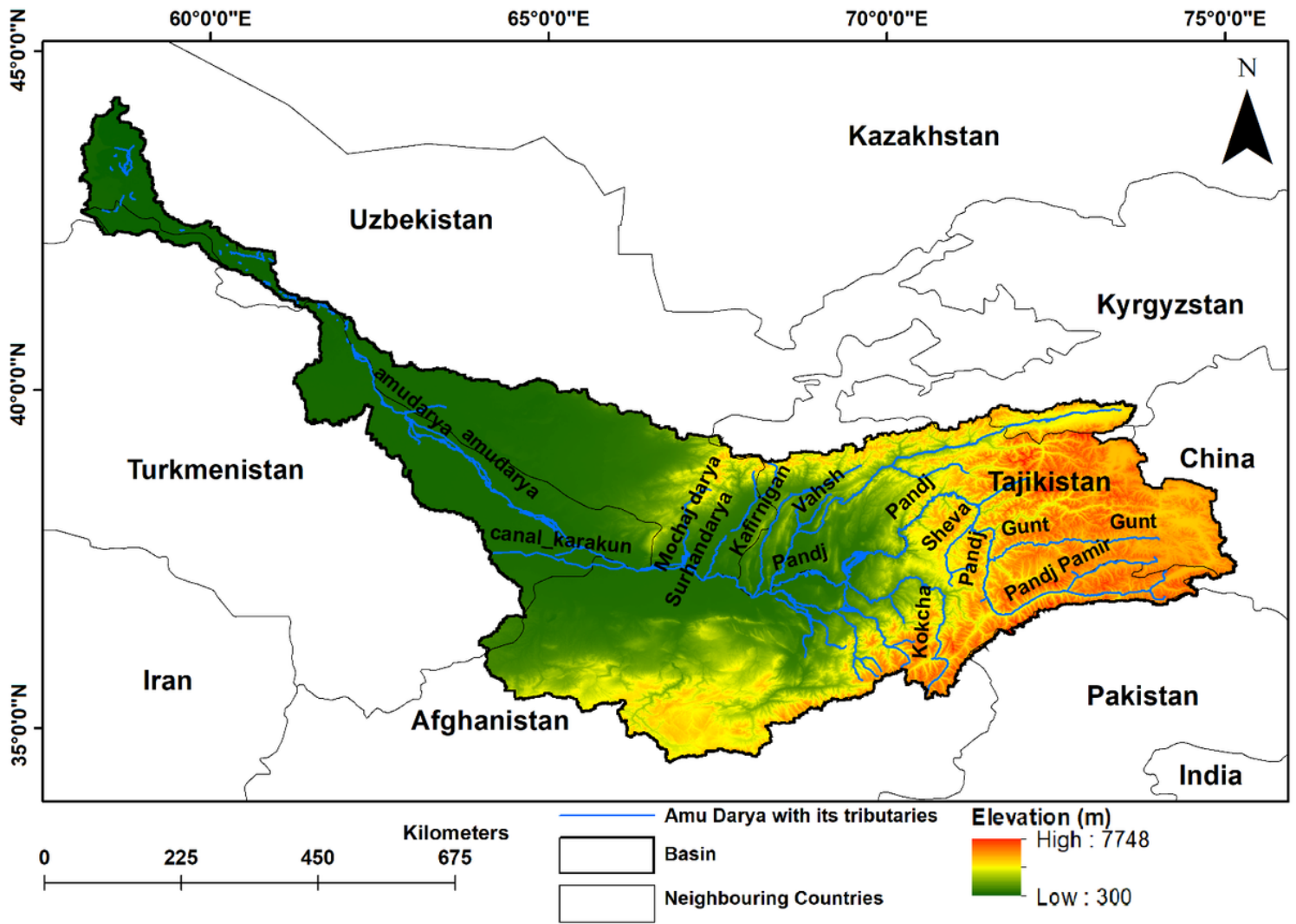
Figures

Figure 1

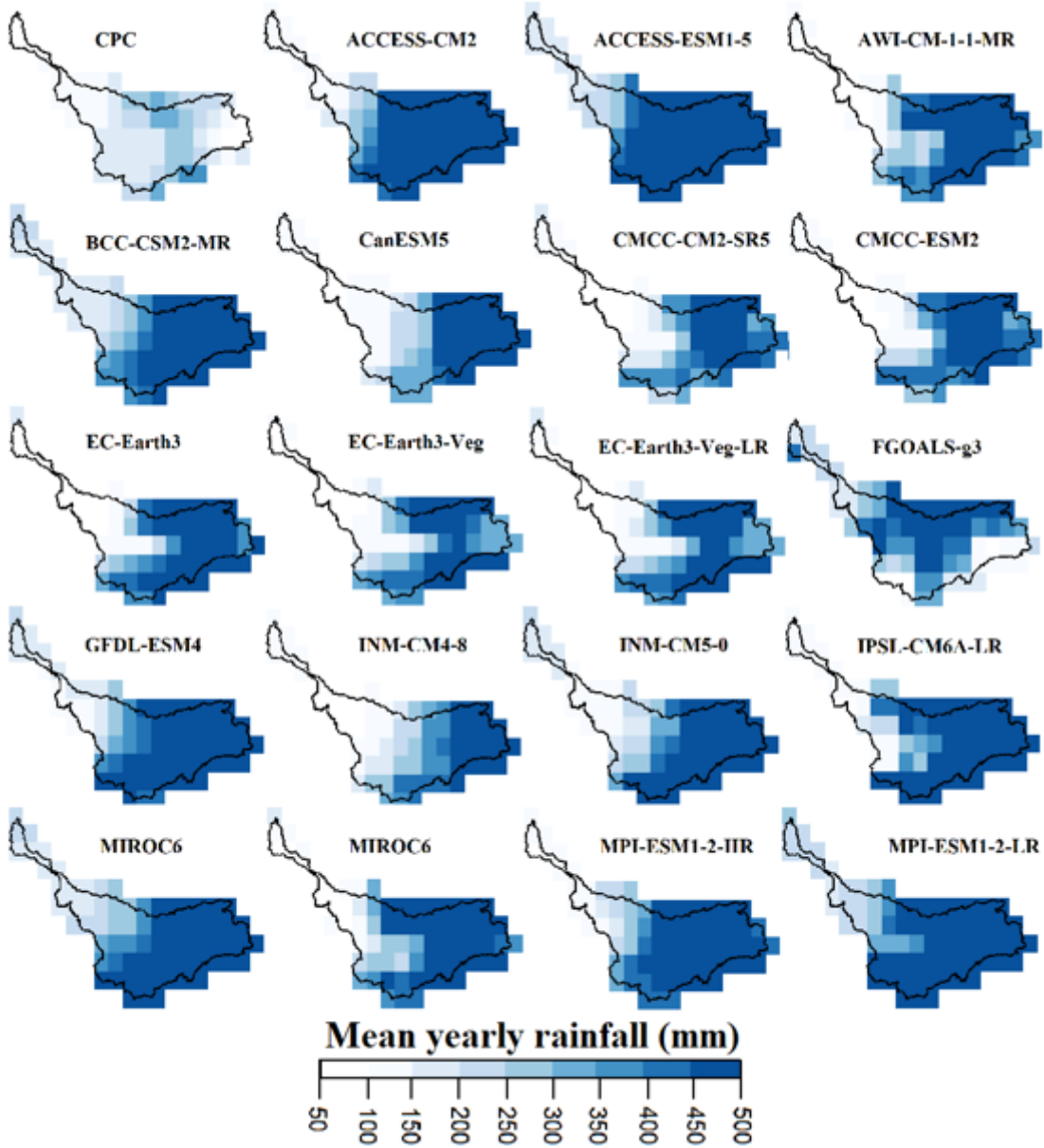The topography of the study region and its location.

Figure 2

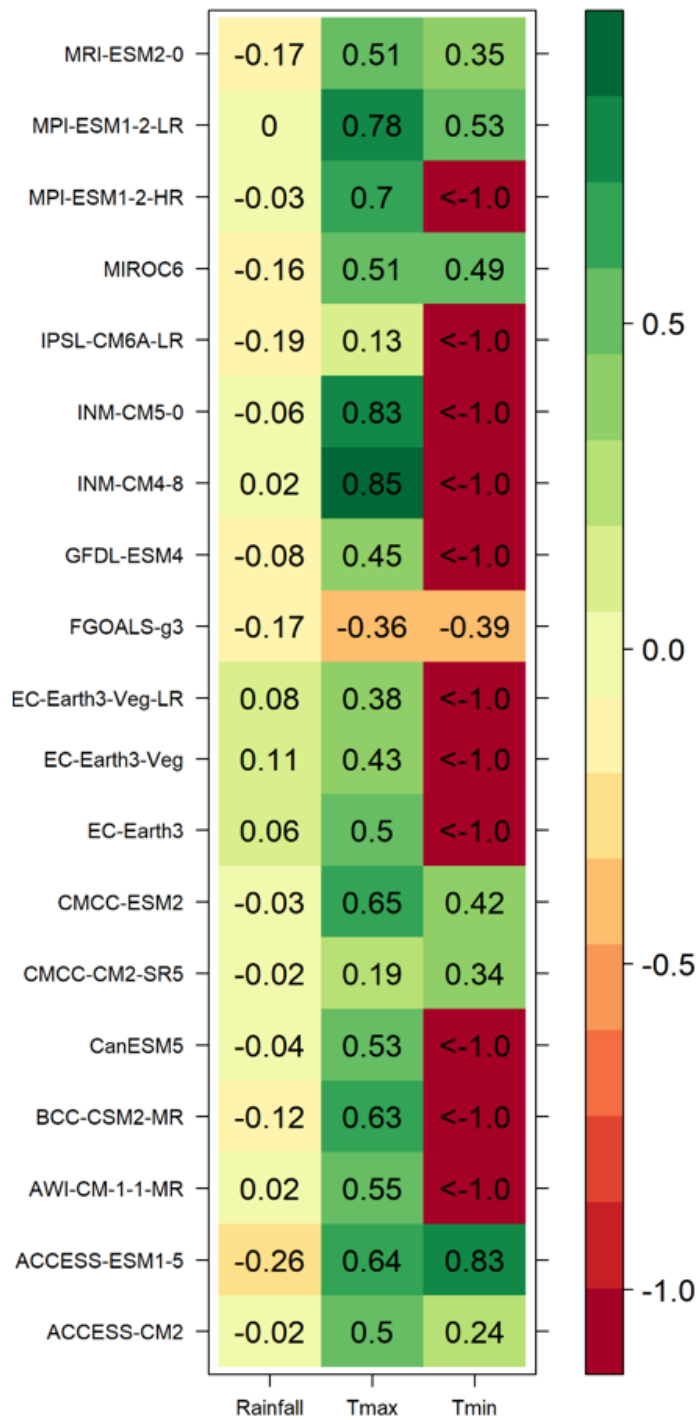Average annual precipitation of GCMs and CPC for the period of 1979-2014.

Figure 3

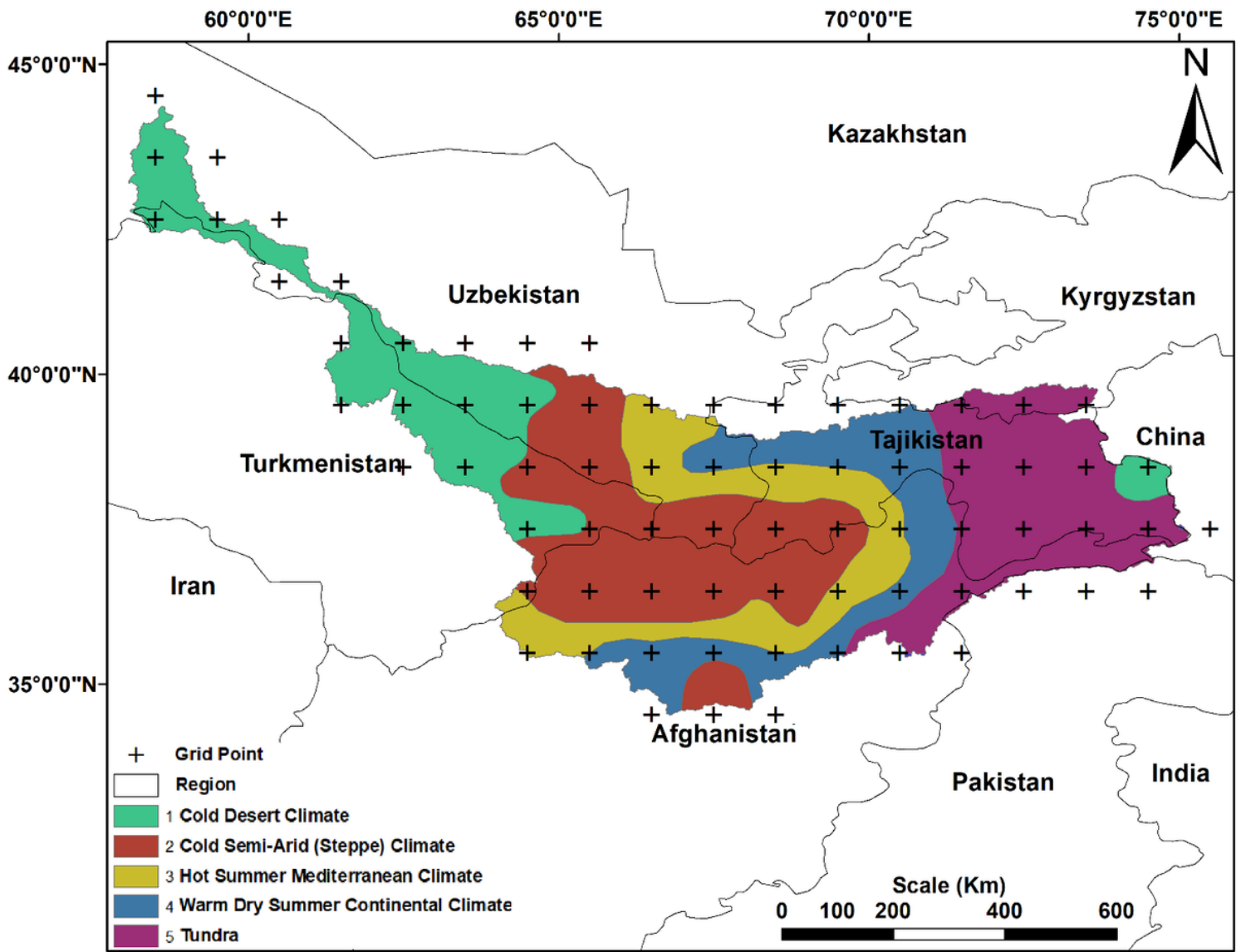Performance evaluation of GCMs rainfall, maximum and minimum temperature using KGE.

Figure 4

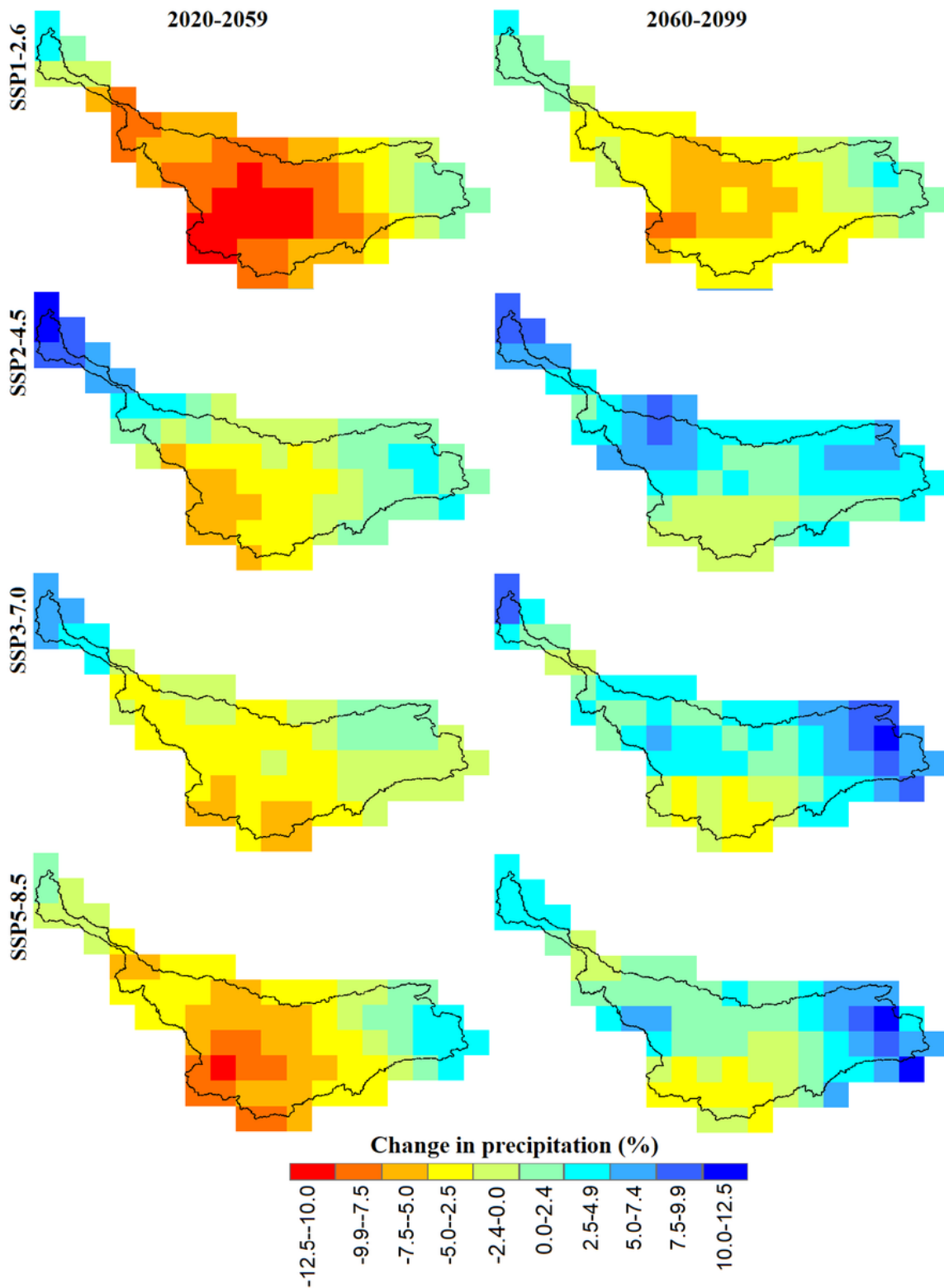Climatic zones of Amu Darya river basin and the climate grid points (1°×1°) over the basin

Figure 5

Spatial patterns in annual precipitation change over the Amu Darya River basin estimated using MME of GCM for the near (2020-2059) and far future (2060-2099) compared to the historical base (1979-2014) for different SSPs.
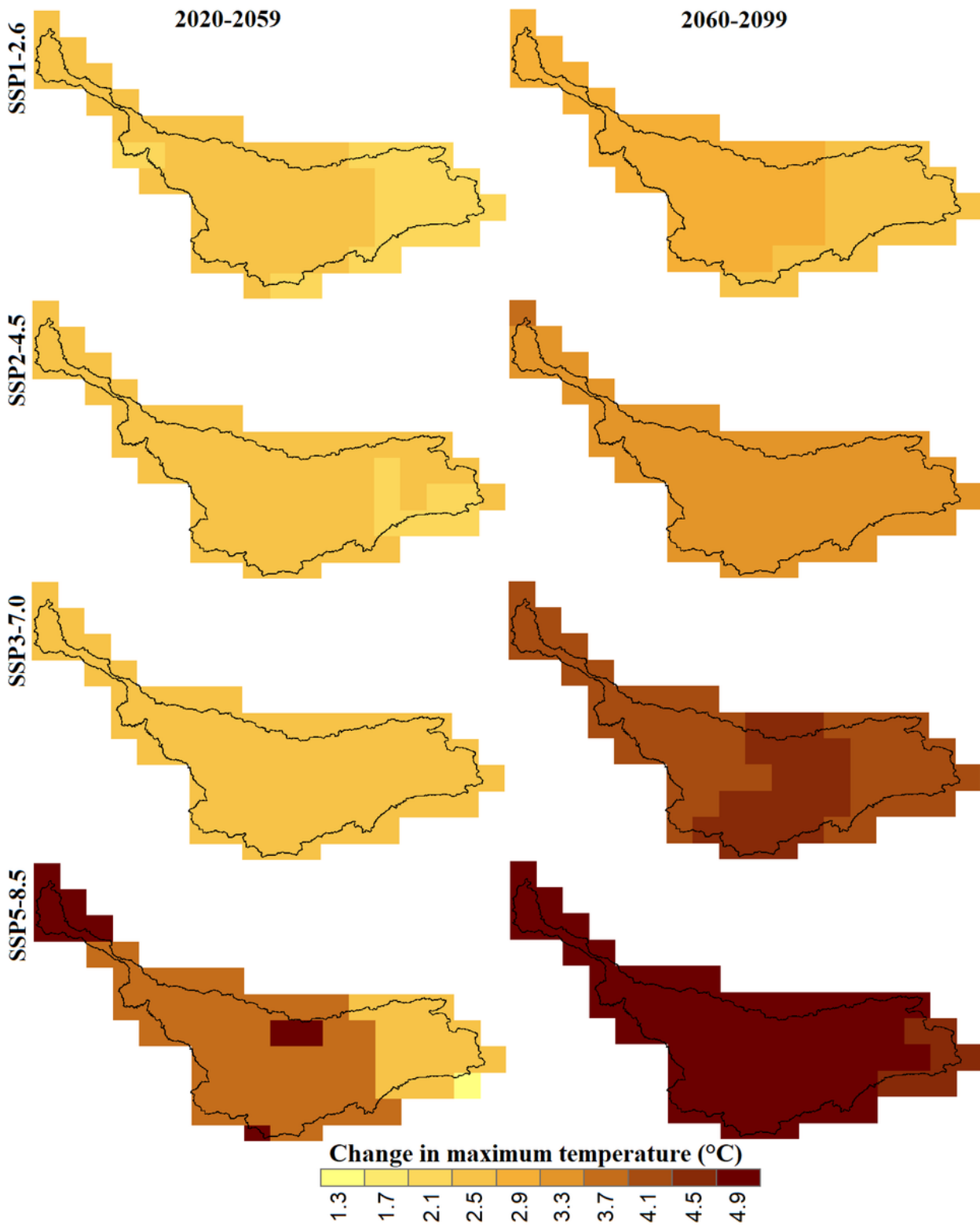
Figure 6

Same as Figure 5, but for Tmx
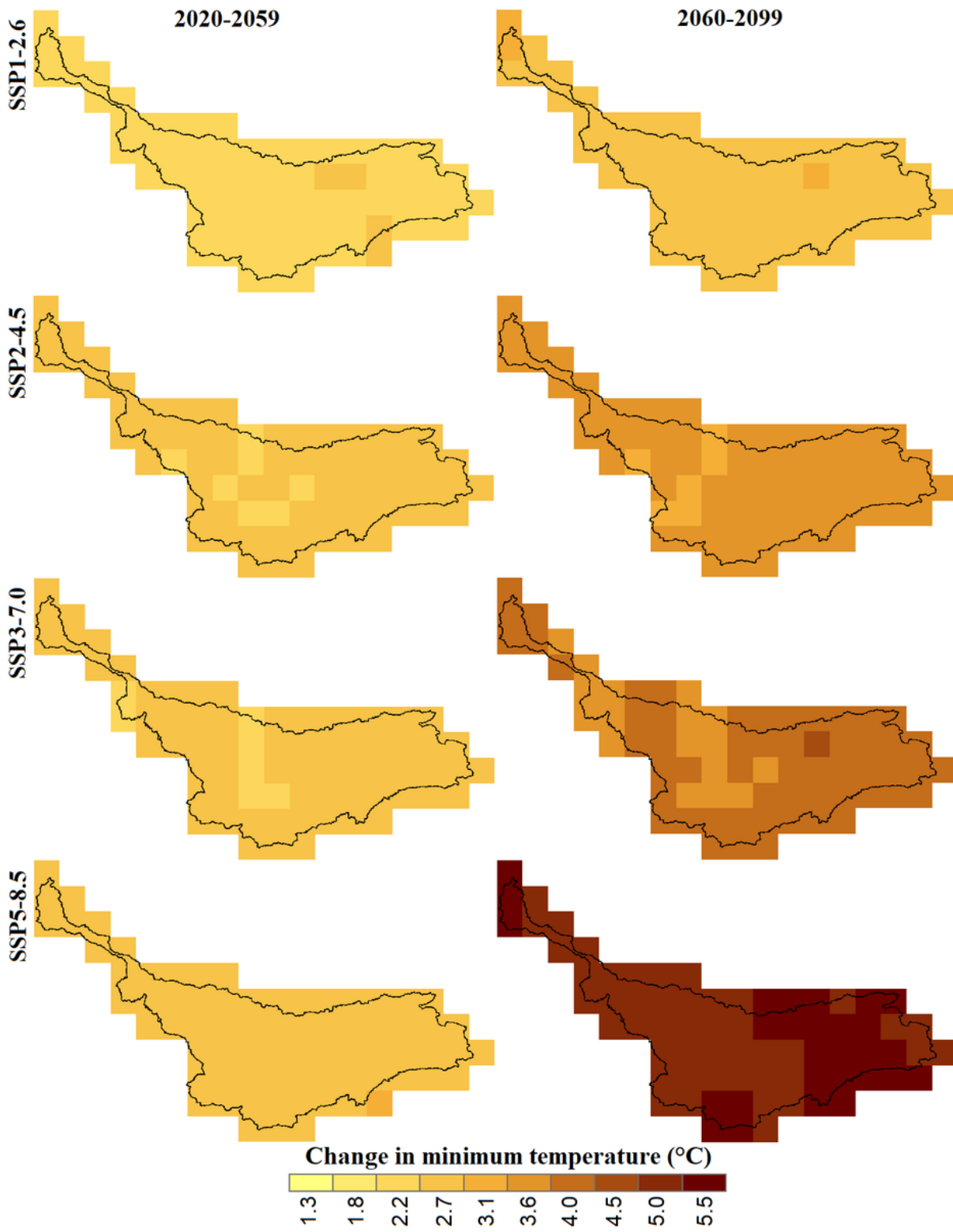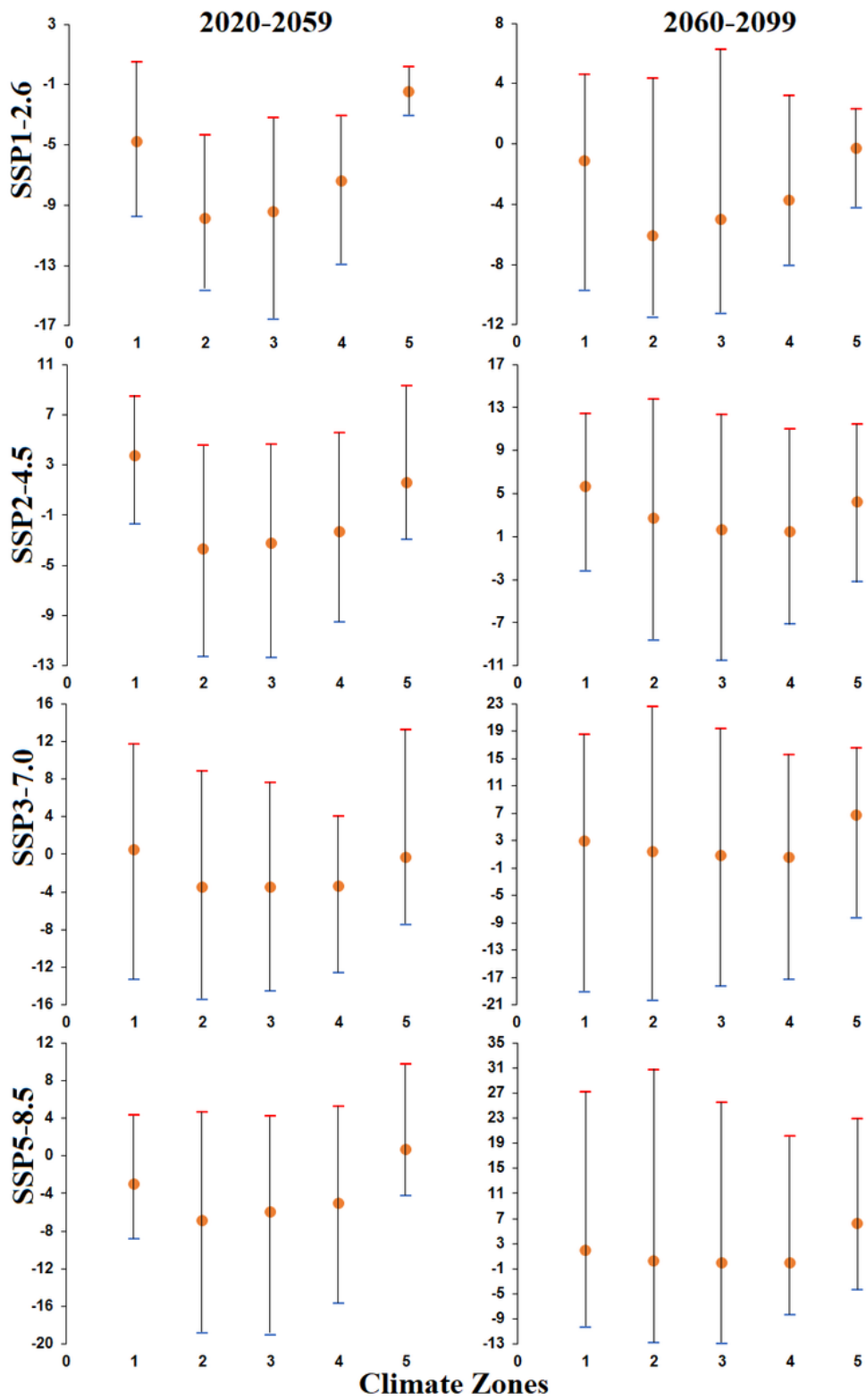
Figure 7

Same as Figure 5, but for Tmn

Figure 8

Uncertainty in the precipitation projected changes (%) in different climatic zones of the Amu Darya basin for two future periods for different SSPs.
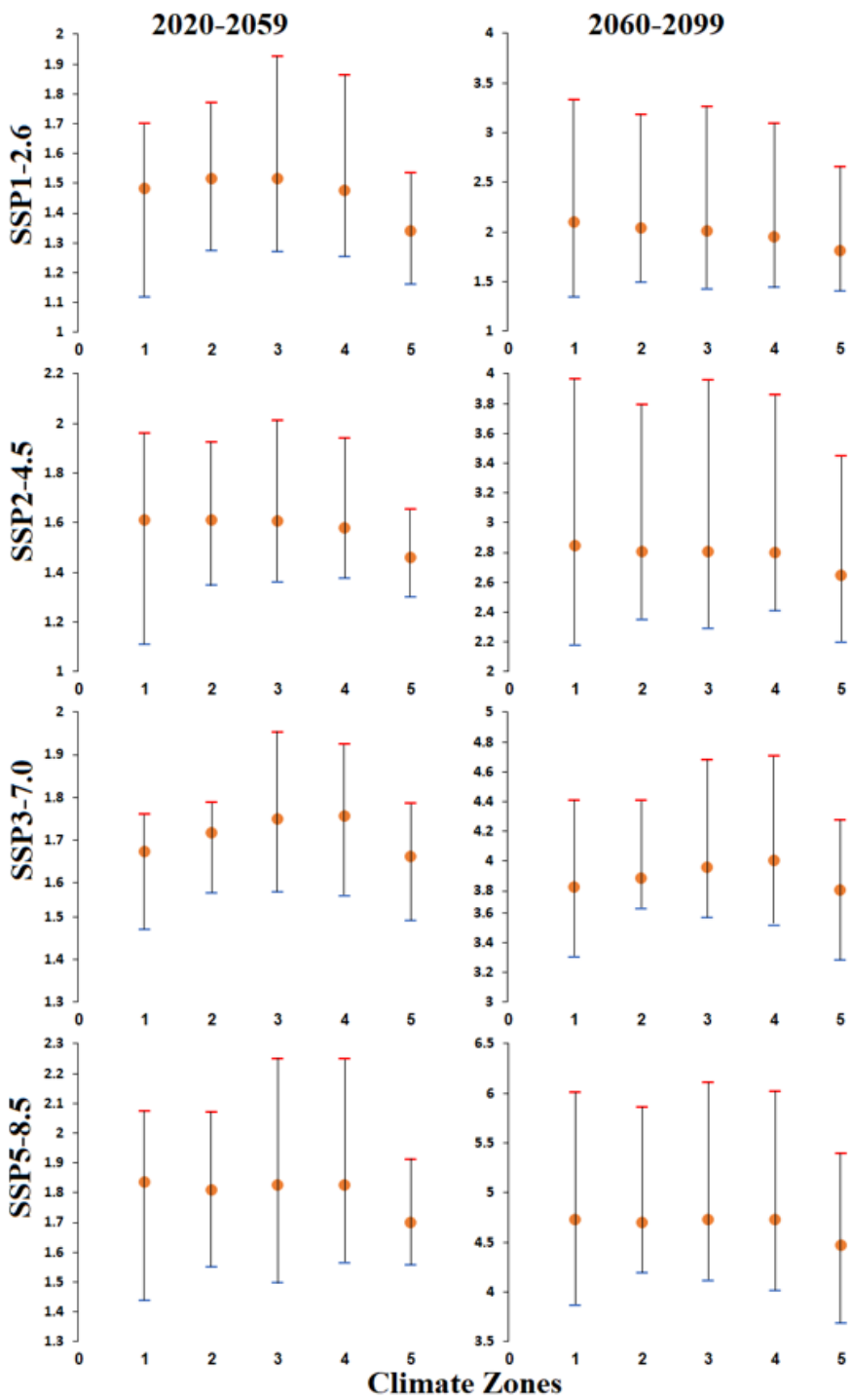
Figure 9

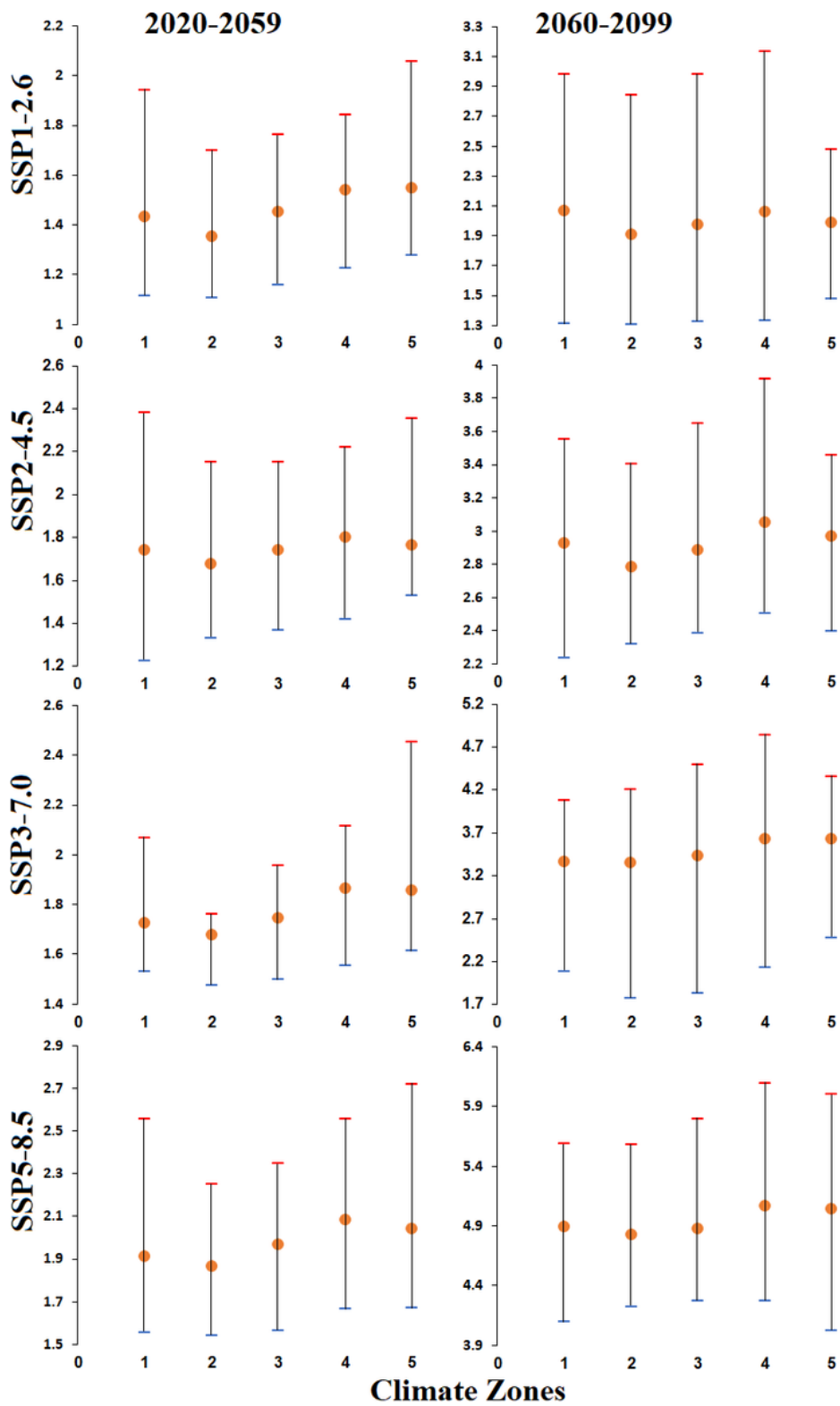Same as Figure 8, but for projected changes (°C) in maximum temperature.

Figure 10

Same as Figure 8, but for projected changes (°C) in minimum temperature.

Supplementary Files

This is a list of supplementary files associated with this preprint. Click to download.

- SupplementaryMaterials.docx